Infrared Physics & Technology 134 (2023) 104873

Contents lists available at ScienceDirect

Infrared Physics and Technology

journal homepage: www.elsevier.com/locate/infrared

Compact diode-pumped tunable single- and dual-wavelength single-frequency semiconductor disk lasers

Mengyuan Xiong [a], Yuquan Zhao [a], Dong Wang [a], Zhong Chen [a], Bin Xu [a,*], Shengjie Yu [b], Cunzhu Tong [b,*]

[a] School of Electronic Science and Engineering, Xiamen University, Xiamen 361005, China
[b] State Key Laboratory of Luminescence and Applications, Changchun Institute of Optics, Fine Mechanics and Physics, Chinese Academy of Sciences, Changchun 130033, China

ARTICLE INFO

Keywords:
Semiconductor disk laser
Single frequency
Dual wavelength

ABSTRACT

Optically pumped external cavity semiconductor disk laser (SDL) combines the characteristics of semiconductor laser and solid-state laser, and has important research value. In this paper, an InGaAs SDL with different emission peak from others was designed. Under free-running operation and a cooling temperature of 12 °C, a few-longitudinal-mode continuous wave laser at 1037 nm with a maximum output power of 2.53 W and a slope efficiency of 41.3% with respect to an absorbed power of about 8.0 W was achieved. Based on this experiment, stable single-wavelength single frequency SDL with maximum output power of 1.79 W was obtained by inserting an etalon into the laser resonator. The single frequency laser was measured to have near-diffraction-limited beam quality. Flexible and continuous wavelength tuning from 1034.77 nm to 1041.10 nm of the single-wavelength single frequency SDL was also realized by introducing another etalon. Under this situation, we also obtained tunable dual-wavelength single frequency SDLs, for the first time to our knowledge. Compared to complex methods such as particular bandgap engineering design or multi-SDL resonator for generating dual-wavelength lasers, the method proposed in this work by using etalons is a simple, feasible, and low-cost solution.

1. Introduction

All solid-state bulk lasers pumped by semiconductor lasers typically use various laser crystals and ceramics as working materials. These lasers have advantages such as robustness, compact structure, high efficiency, high reliability, long lifespan, easy operation, and low cost. However, the output performance of solid-state bulk lasers is influenced by many factors. For example, when the quality of the pump light beam is relatively poor, due to the gain medium having a certain size in the propagation direction of the pump light, the mode overlap efficiency of the pump beam and cavity mode is very low, resulting in low laser efficiency. In addition, solid-state bulk laser is prone to form strong thermal lensing effect, which not only limits the output power of the laser, but also leads to poor beam quality of the output laser. Generally, it is difficult to obtain TEM_{00} mode laser output, which is very unfavorable for the application of lasers. Therefore, solid-state disk lasers with very thin crystals as gain media have emerged, which effectively solve the aforementioned problems of solid-state lasers. However, new problems also arise: due to the small absorption coefficient of crystal or ceramic materials and the very thin thickness of the disk, in order to achieve sufficient absorption of the pump laser, a very complex multi-pass pump structure needs to be used. For solid-state lasers, another prominent issue is that their lasing wavelength is limited by active ions.

Compared to edge emitting semiconductor lasers, the advantage of vertical cavity surface emitting lasers (VCSELs) is that they can achieve diffraction limited beam quality. VCSEL is indeed a semiconductor material disk, and therefore theoretically it has advantages of power scaling and high beam quality as crystal disk lasers have. Although it is also very thin, due to the high absorption coefficient of semiconductors, this type of disk can have high absorption of pump light without the need for complex multi-pass absorption structures. Moreover, VCSEL can theoretically achieve a rich range of lasing wavelengths by adjusting semiconductor materials and structural design (band engineering), which can compensate for the shortcomings of conventional solid-state lasers.

When replacing the crystal disk with a VCSEL as gain medium in an

* Corresponding authors.
E-mail addresses: xubin@xmu.edu.cn (B. Xu), tongcz@ciomp.ac.cn (C. Tong).

https://doi.org/10.1016/j.infrared.2023.104873
Received 18 June 2023; Received in revised form 9 August 2023; Accepted 22 August 2023
Available online 24 August 2023

external cavity configuration and pumping it with a diode laser, it becomes optically pumped semiconductor (OPS) vertical-external-cavity surface-emitting laser (VECSEL, i.e. SDL). This new laser technology, which combines the technologies of solid-state laser and semiconductor laser, has been developed for more than 20 years since Kuznetsov et al. presented the first demonstration in 1997 [1]. At present, in addition to mode-locked SDL [2–6], which has been mostly investigated, the research on single-frequency SDL has also received attention. For example, in 1999, Holm et al. reported a 42-mW single frequency SDL at about 870 nm [7]. In 2006, Jacquemet et al. reported a 500-mW single frequency SDL at 1003.4 nm and its frequency doubling to 501.7 nm with an output power 62 mW [8]. In 2009, Laurain et al. presented a 0.3-W free-run single frequency SDL at 1.02 μm based on a short cavity (less than3 mm) configuration [9]. One year later, researchers from the same group improved the output power to 2.1 W by using a pump source with higher power and this time the authors found that single frequency lasing can still be achieved when the cavity was lengthened to 10 mm [10]. Rantamaki et al. [11] achieved a 4.6-W single frequency SDL at around 1.05 μm. In 2014, Zhang et al. reported a single-frequency SDL at 1013 nm with a record output power of 23.6 W [12].

Although there have been some researches on single frequency SDLs, there are few studies involving active wavelength tuning of single frequency SDLs, and studies involving dual-wavelength single frequency SDLs have not yet been reported, to the best of our knowledge. In fact, dual-wavelength SDLs have ever been reported several times [13–16], however they are not operated in single frequency modes. Practically, compact dual-wavelength single-frequency lasers have important applications, such as in generating millimeter or microwave signals via optical beating technique [17] and differential Lidar system [18].

In this work, by designing an InGaAs SDL with lasing peak at around 1037 nm, i.e. different from other single-frequency SDLs as mentioned above, and using an 808-nm diode laser as pump source, we have operated simple, compact and stable single-frequency SDLs under the help of F-P etalons. Moreover, whether it is single-wavelength or dual-wavelength single frequency SDL as we obtained in the experiments, they all exhibited good flexibility in wavelength tuning. In addition, these single frequency SDLs show great beam qualities with M^2 factors close to diffraction limit.

2. Experimental details

In Fig. 1, we present the schematic diagram of the diode-pumped single-frequency SDL. Firstly, the pump source is a fiber-coupled 808 nm semiconductor laser with a core diameter of 105 μm and a numerical aperture of 0.15. The maximum output power of the pump source is 12 W. In the experiment, two lenses with focal lengths of 30 and 40 mm were respectively used to collimate the pump beam. A lens with a focal length of 100 mm was used to focus the pump beam. Thus, the combination of different collimating lenses and the same focusing lens will result in different pump spot sizes in the gain material. The pump laser strikes the semiconductor gain disk at an incidence angle of approximately 30°. Due to the lack of antireflection on the semiconductor surface, approximately one-third of the pump power is reflected off the surface of the semiconductor material, resulting in a maximum absorbed pump power of about 8 W in the experiments. Using several concave mirrors with the same curvature radius of 100 mm and different transmissions to couple the cavity mode laser out of the resonator, we have further explored the output power performance of the disk laser.

The structure of the SDL used in this work is the same as we used previously in Ref. [19]. It is composed of an active region with semiconductor quantum-wells (QWs), distributed Bragg reflector (DBR) mirror and InGaP cap layer. It is grown in reverse order on GaAs substrates through metal organic vapor phase epitaxy (MOVPE). The DBR mirror is made up of 20 pairs of undoped AlAs/GaAs layers in order to have high reflectivity for target wavelengths. The active region includes 10 layers of 8 nm InGaAs compressively strained QWs with GaAs barrier and a tensile strained GaAsP layer for strain compensation. Fig. 2(a) shows those QWs, which are distributed periodically at the optimized anti-node positions of the standing wave in the optical cavity to ensure a low threshold and homogeneous gain. Afterwards, there is a half wavelength InGaP cap layer to prevent carrier diffusion to the chip surface and to prevent nonradiative recombination there. The chip was bonded to a diamond heat spreader by pre-metallized diamond method and the substrate was removed by selective chemical etching. Fig. 2(b) shows the semiconductor disk after a series of treatments of pre-metallization. Moreover, due to the significant relationship between the output characteristics of semiconductor laser and temperature, as well as the need to consider thermal effects, we directly bonded this packaged semiconductor disk to a water-cooled copper block by welding, and set the temperature of the water-cooling chiller to 12 °C. We used etalons to narrow the laser linewidth in order to obtain single frequency lasers while also ensuring good stability of the output lasers.

3. Results and discussion

In Fig. 2(c), we show the photoluminescence spectrum of the

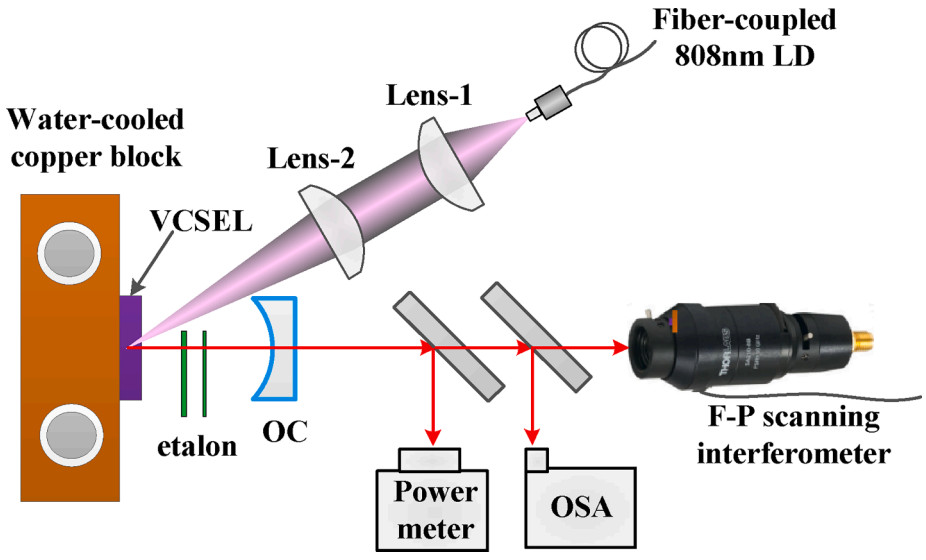

Fig. 1. Schematic of experimental setup of diode-pumped single-frequency semiconductor disk lasers.

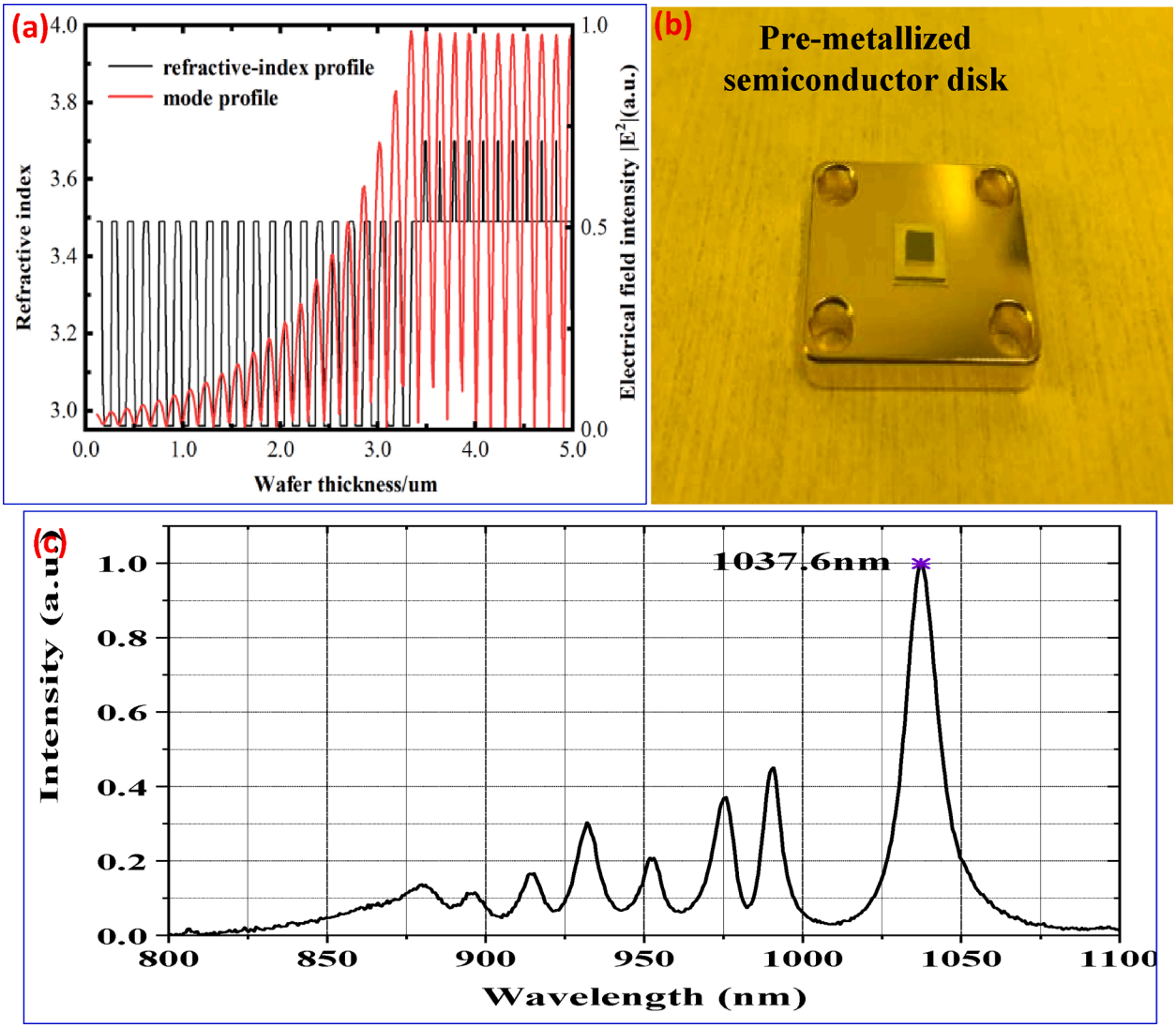

Fig. 2. (a) The refractive index profile and the standing wave distribution in the active region of the designed SDL, (b) picture of the semiconductor disk after the treatment of pre-metallization and (c) measured photoluminescence spectrum of the semiconductor disk at cooling temperature.

semiconductor disk at the water-cooled temperature, from which one can see that the main emission peak of the disk is located at 1037.6 nm, with a half width of approximately 10.4 nm. There are about 8 sub peaks at the shorter wavelength, but the intensity and width of these sub peaks are much smaller than the main peak. Therefore, it can be foreseen that the main emission of the disk is around 1037 nm.

Throughout the experiment, the physical length of the laser cavity was maintained at approximately 7 mm. A free running continuous wave laser experiment using the 40-mm collimating lens (and the 100-mm positive lens for focusing) was firstly conducted and the experimental results are shown in Fig. 3(a). Using a 1.8% transmitted OC, the lasing behavior can be found at an absorbed power of about 1.0 W, which is a relatively low threshold situation for semiconductor disk lasers. Increasing the pump power, we achieved a maximum output power of 2.09 W at a maximum absorbed power of 8.11 W, which led to a slope efficiency of about 29.5%. By replacing this lowest transmittance OC with another two OCs with 2.7% and 3.6% transmittances, we obtained maximum output powers of 2.33 W and 2.07 W, respectively, with corresponding slope efficiencies of 38.5% and 41.2%. Comparing these two results, it can be found that the 3.6% OC has higher efficiency, but the maximum output power is lower. This is because the output power shows a significant rollover phenomenon when the absorbed pump power exceeds 6.6 W. Relatively speaking, output power by using the 2.7% OC shows better linearity. Although the slope efficiency decreases when the absorbed pump power exceeds 6.6 W, there is no rollover phenomenon. It could suggest that for the current laser the optimal transmittance of the OC should be a value between 2.7% and 3.6%.

Fig. 3(b) shows the experimental results when using the 30-mm (focal length) lens for collimating the pump beam. In this case, the pump beam waist size (from about 260 μm) increases to 350 μm. A large pump spot size will result in a high laser threshold, but a large pump spot size will also be beneficial for thermal alleviation, which could result in better laser performance. For the OCs with transmittances of 1.8%, 2.7% and 3.6%, we have achieved maximum output powers of 1.81 W, 2.53 W and 2.08 W, respectively. The corresponding slope efficiencies are 27.5%, 41.3% and 38.5%. Under this situation, these three sets of output power data all exhibit good linear characteristics, which is the result of alleviated thermal effect. Even to our surprise, we found that for the 2.7% OC, the maximum power increased from 2.33 W to 2.53 W due to the data at high output powers maintaining the same slope efficiency as at low output powers. This is also the highest output power obtained in this work.

We also evaluated the correlation between the output power of this SDL and the water cooling temperature, as shown in Fig. 3(c). The current maximum power of 2.53 W was obtained at a water cooling temperature of 12 °C. When we lowered the temperature to 6 °C, which

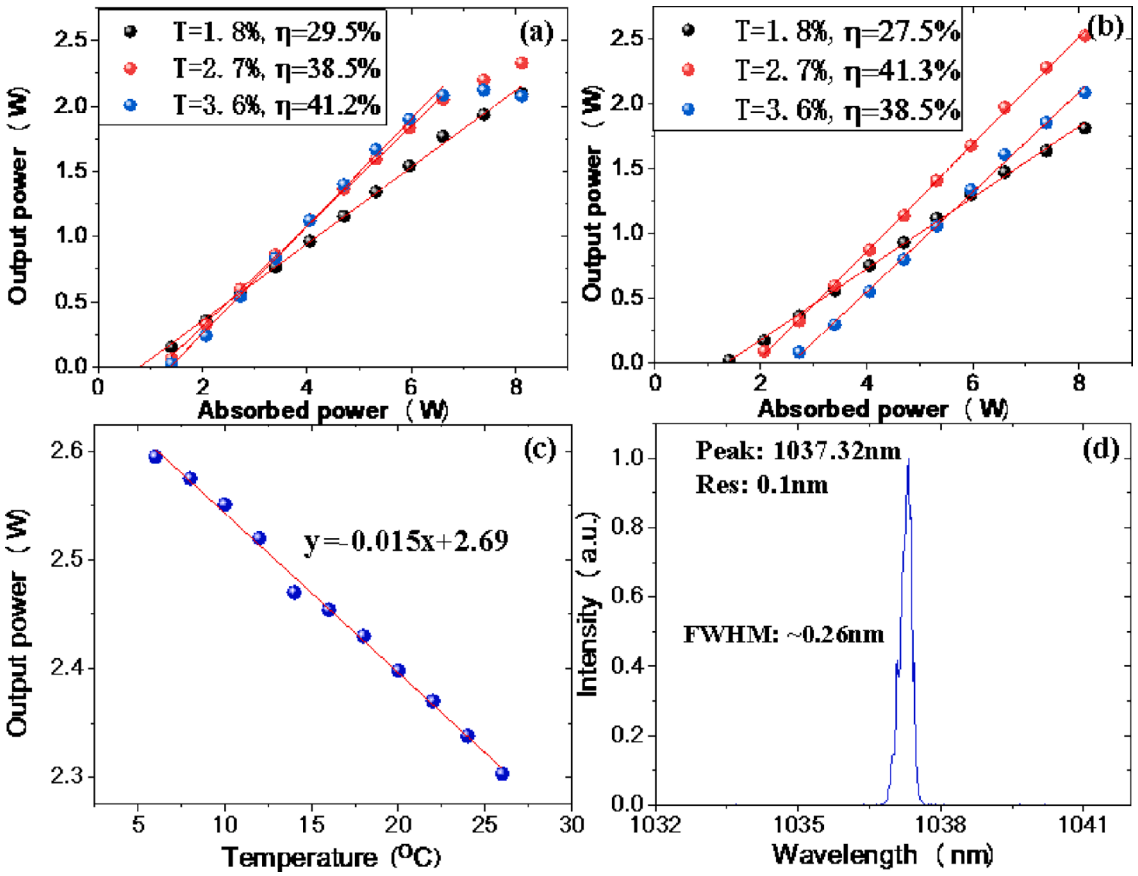

Fig. 3. (a) Output power versus absorbed power of the semiconductor disk laser in free-running operation with a 40-mm (focal length) collimating lens and a 100-mm focusing lens, (b) output power versus absorbed power of the semiconductor disk laser in free-running operation with a 30-mm collimating lens and a 100-mm focusing lens, (c) the maximum output power as a function of temperature and (d) typical laser spectrum under free-running operation with a peak at 1037.32 nm.

was the lowest temperature to ensure that no water condensation was formed on the disk in the experimental environment at that time, we found that the output power increased to 2.60 W. The output power decreased to 2.30 W when we set the water cooling temperature to the highest of 26 °C. Therefore, by linearly fitting the data shown in Fig. 3 (c), we can conclude that for every 1 °C change in temperature, the output power of the laser changes by 0.015 W. Or in other words, the thermal resistance is approximately 66.67 K/W. A very small ratio of power variation with temperature is very advantageous for the application of this SDL, especially in situations where the temperature changes significantly. It should be pointed out that although we fixed the pre-metallized semiconductor disk and water-cooled copper block together through welding, and due to the low pump power in the experiment, no significant temperature difference was found. However, since the semiconductor disk did not adopt active temperature control, the output power varying from temperature measured here may need to be further verified after more accurate temperature control and measurement.

At the highest output power, using an optical spectrum analyzer with resolution of 0.1 nm, we measured the laser spectrum as shown in Fig. 3 (d). It can be seen that the peak wavelength of the laser is 1037.32 nm, and the full width at half value of the laser wavelength is about 0.26 nm. Since the semiconductor disk is very thin, the influence of its high refractive index (about 3.0) on the longitudinal mode spacing in the cavity can be ignored. As a result, we calculate that the longitudinal mode spacing is about 0.077 nm. In this way, the 0.26-nm linewidth corresponds to approximately three longitudinal modes. So, this is indeed a few-longitudinal-mode laser, which should thank to the short laser resonator providing a large free spectral range. According to the theoretical calculation, a cavity with length of about less than 3 mm could lead to single frequency laser generation in free-running mode [9]. Moreover, we found that by adjusting the orientation of the OC, therefore adjusting the resonator loss, single-longitudinal-mode operation can also be achieved. But in this case, the stability of the single frequency is not satisfying, always hopping between single longitudinal mode and few longitudinal modes.

The above results have prompted us to further achieve stable single longitudinal mode laser operation. We therefore placed a thin BK-7 plate with a thickness of approximately 0.1 mm into the laser cavity, which plays a role as F-P etalon and has been demonstrated previously for single-frequency laser generation [20] and wavelength tuning [21]. Fig. 4 shows the experimental results after inserting the etalon. We only used the 2.7% OC, i.e. the one we achieved the highest output power in the above experiment, to carry out the single-frequency laser experiment. The introduced insertion loss is not significant and does not result in a significant increase in the laser threshold. We estimated the insertion loss of the etalon by using this expression as $L = 2\theta Rd/nw$ [22], where θ is the incident angle, R is the etalon reflectivity for the angle θ, d the thickness, n the refractive index, and w the beam waist radius onto the etalon. The calculated insertion loss is approximately on the order of less than 0.3%. However, the maximum output power has decreased to 1.79 W (see Fig. 4(a)), which is approximately 29% lower than the previous maximum power of 2.53 W. This may be due to the etalon inserted into the laser cavity at a very small angle, and in this case, the transmission of the etalon for the laser is not 100%, thus introducing losses. The slope efficiency of the laser is linearly fitted to be about 29.6% with respect to the absorbed power.

In Fig. 4(a), we also show the laser wavelength peaking at 1037.08 nm with a FWHM of about 0.078 nm. Due to the laser resolution being only 0.1 nm, the measured linewidth is very likely to be limited by the

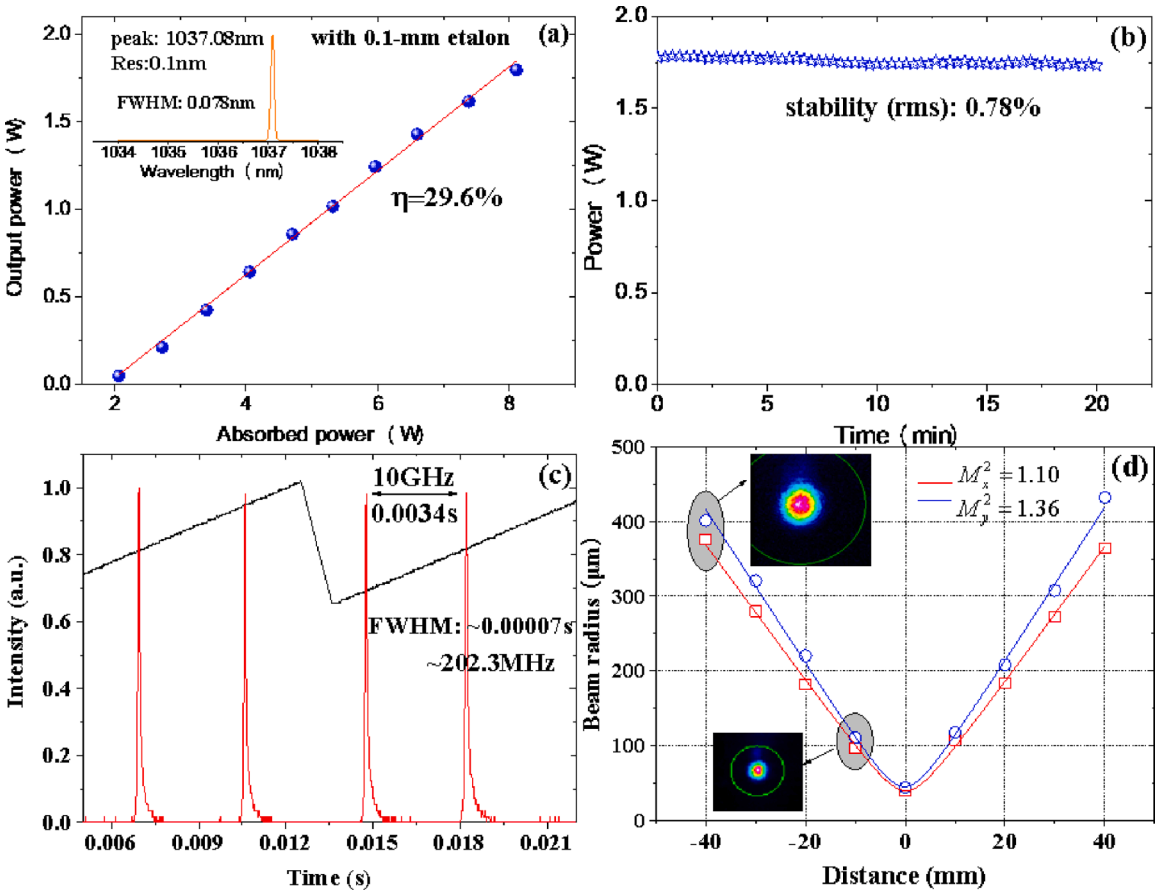

Fig. 4. (a) Output power versus absorbed power when the 0.1-mm etalon was inserted into the cavity and the corresponding laser spectrum with peak at 1037.08 nm, (b) power stability of the 1037.08 nm single frequency laser, (c) F-P interferometer scanning spectrum and (d) beam radius at different distance for assessing the M^2 factor of the SDL.

resolution. In addition, in Fig. 4(b), we show the maximum output power stability of the achieved laser within 20 min and a stability value (RMS) of about 0.78% can be found. In comparison to the free-running laser operation, the present stability of the laser was greatly improved. In order to check the longitudinal mode property, we injected the output laser into an F-P scanning interferometer (SA210-8B, Thorlabs Inc.). The result is reported in Fig. 4(c), which clearly indicates the present laser operating in single longitudinal mode. Moreover, its linewidth is found to be about 202.3 MHz. Since the used F-P scanning interferometer has a resolution of 67 MHz, the measured linewidth is basically reliable. The linewidth corresponds to a wavelength FWHM of approximately 0.00072 nm at this wavelength, which is far less than the value that we measured using the optical spectral analyzer. More accurate measurement of laser linewidth may require the use of other means, such as commonly used delayed self-heterodyne method [23]. A small beam spot can be observed far from the OC by using an infrared sensor card, which should indicate a small divergence angle of the output laser and a good beam quality. We then injected the single frequency laser beam into a focusing lens with a focal length of 50 mm and then used a WinCamD-LCM CMOS beam profiling camera (DataRay Inc.) to measure the size of the spot before and after the focusing position. The results are shown in Fig. 4(d). By fitting the data with the expression of beam propagation factor M^2, we can deduce that the M^2 factors of the output laser in the *x* and *y* directions are 1.10 and 1.36, respectively, indicating that the single frequency laser has excellent beam quality near the diffraction limit. It is well-known that multi-longitudinal mode and high-order transverse mode are important causes of laser instability. Therefore, from this point of view, single longitudinal mode laser with fundamental mode beam quality obtained in this experiment is an important stability guarantee of the output laser.

In theory, in comparison to single etalon, dual etalons combination exhibits more powerful capacity in wavelength discrimination and linewidth narrowing. In the experiment, the relevant investigation was further fulfilled by inserting another etalon with a thickness of 0.5 mm into the laser resonant cavity. Under this situation, the cavity was a little bit lengthened for flexibly tilting the etalons. According to the transmission expression of etalon [24], we simulate the transmission curves, as shown in Fig. 5(a). It can be seen that at 1037.08 nm the transmission is 100% induced by the two etalons. Moreover, by finely tilting the angles of the two etalons to form different angle combinations, the maximum transmission can shift to other low-gain wavelengths and resultingly generate large losses on high-gain wavelengths. Using this method, we not only achieved wavelength tuning of the single-wavelength single frequency laser, but also further achieved tunable dual-wavelength single frequency laser. The drawback is that inserting another etalon will cause extra round-trip loss. According to the above expression we can estimate that the relatively thick etalon will introduce an additional intracavity loss of 1.5% if we don't consider the slight changes in the size of the beam spot. Fig. 5(b) shows the single-wavelength single frequency laser wavelengths obtained in this experiment from 1034.77 nm to 1041.10 nm with their corresponding output powers. Fig. 5(c) shows the achieved dual-wavelength single frequency lasers with different combinations as 1034.70 + 1037.28 nm, 1036.12 + 1038.72 nm, 1036.80 + 1039.36 nm, 1037.00 + 1039.48 nm and 1037.48 + 1040.00 nm. During the experiment, we made efforts to maintain the two wavelengths with similar intensities as much as possible by finely tilting the angles of the two etalons (see in Fig. 5(c)). We also measured the spectral characteristics of these single frequency

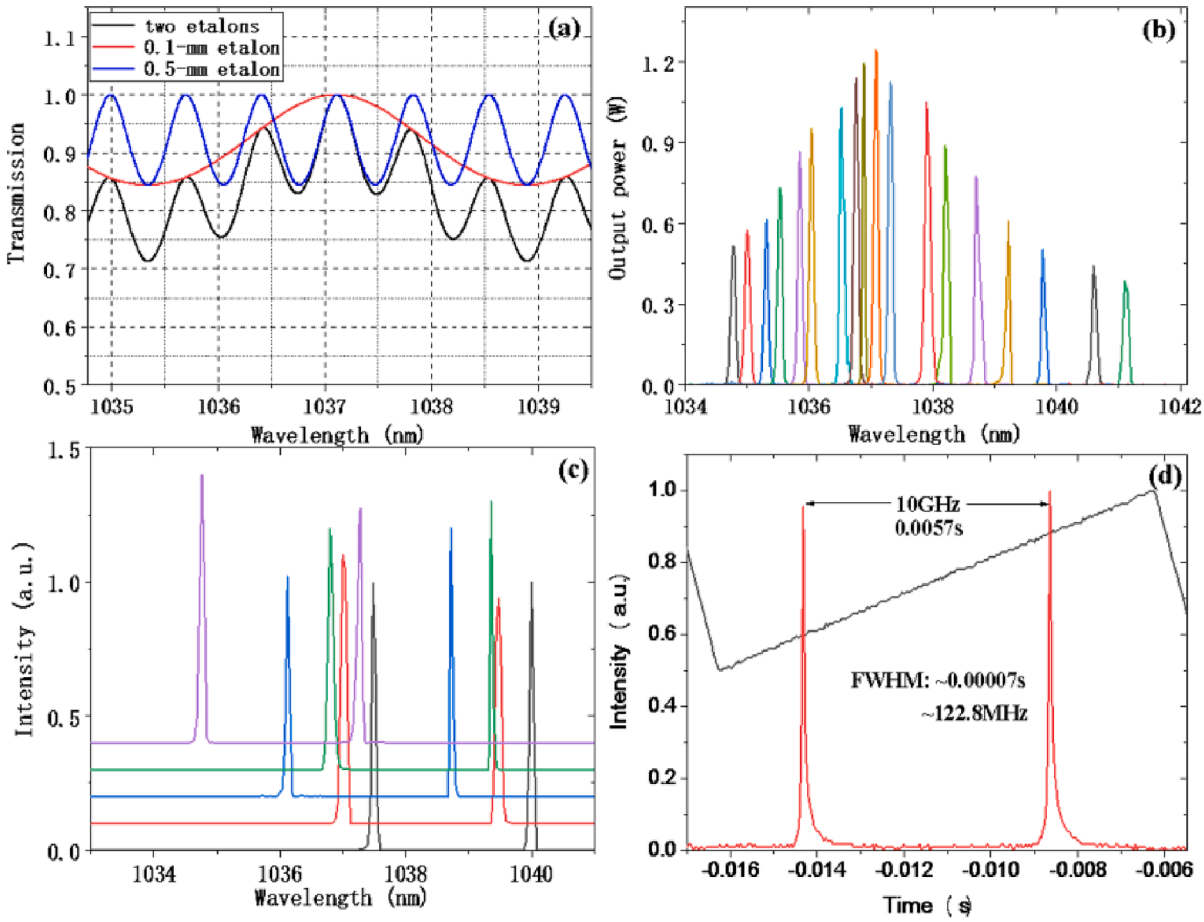

Fig. 5. (a) Transmission curves of the etalons at considered wavelengths, (b) tunable single-wavelength single-frequency lasers and their corresponding maximum output powers, (c) tunable dual-wavelength single-frequency lasers and (d) typical F-P interferometer scanning spectrum of a dual-wavelength single-frequency laser.

lasers by using the F-P scanning interferometer. Fig. 5(d) is a typical measurement result of the 1034.70 + 1037.28 nm laser at maximum output power of 635 mW. According to this measurement, the linewidth was estimated to be about 122.8 MHz, i.e. about 0.00043 nm, which is a much narrower linewidth than that we achieved for a single-wavelength single-frequency laser. Obviously, the newly inserted etalon further narrowed the laser linewidth. In addition, basically, the stabilities of these dual-wavelength single frequency lasers are worse than that of single-wavelength single frequency lasers, for example, the stability of 1034.70 + 1037.28 nm single frequency laser measured within 20 min is about 0.92%. The relatively degraded stability should be due to longitudinal mode competition between the two wavelengths.

Last but not least, whether for single-wavelength or dual-wavelength single frequency lasers, mode hopping phenomenon exists, mainly due to air disturbance and mechanical vibration in our laboratory environment. This mode hopping can be greatly improved through strict sealing and modular design of the laser prototype.

4. Conclusion

By constructing a simple and compact external cavity SDL, we obtained a 2.53 W continuous wave laser that operates in few longitudinal modes. Under the help of a 0.1-mm etalon, single-wavelength single frequency laser at 1037.08 nm was also realized with a maximum output power of 1.79 W. By inserting another etalon with thickness of 0.5 mm, we achieved tunable single-wavelength single frequency laser with a range of about 7 nm and tunable dual-wavelength single frequency lasers. In the near future, whether for single-wavelength or dual-wavelength single frequency lasers, we will be committed to significantly increasing the output power of these single frequency lasers while also narrowing the linewidth of single frequency lasers to the domain of kHz through feedback technology. Moreover, with the help of feedback technology, the frequency stabilization of the single frequency lasers will also be more reliable, eliminating the occurrence of mode hopping.

Declaration of Competing Interest

The authors declare that they have no known competing financial interests or personal relationships that could have appeared to influence the work reported in this paper.

Data availability

Data will be made available on request.

Acknowledgments

This work was supported by National Science Fund for Distinguished Young Scholars (62025506), Natural Science Foundation of Xiamen of China (3502Z20227166), Program of State Key Laboratory of Quantum Optics and Quantum Optics Devices (KF202102) and Key Laboratory of OptoElectronic Science and Technology for Medicine of Ministry of Education and Fujian Provincial Key Laboratory of Photonics Technology (JYG2003).

References

[1] M. Kuznetsov, I.E.E.E. Member, F. Hakimi, R. Sprague, A. Mooradian, High-Power (>0.5-W CW) Diode-Pumped Vertical-External-Cavity Surface-Emitting Semiconductor Lasers with Circular TEM_{00} Beams, IEEE Photon. Technol. Lett. 9 (8) (1997) 1063–1065.

[2] S. Hoogland, S. Dhanjal, A.C. Tropper, J.S. Roberts, R. Häring, R. Paschotta, F. Morier-Genoud, U. Keller, Passively Mode-Locked Diode-Pumped Surface-Emitting Semiconductor Laser, IEEE Photon. Technol. Lett. 12 (9) (2000) 1135–1137.

[3] A. Garnache, S. Hoogland, A.C. Tropper, I. Sagnes, G. Saint-Girons, J.S. Roberts, Sub-500-fs soliton-like pulse in a passively mode-locked broadband surface-emitting laser with 100 mW average power, Appl. Phys. Lett. 80 (21) (2002) 3892–3895.

[4] A.H. Quarterman, K.G. Wilcox, V. Apostolopoulos, Z. Mihoubi, S.P. Elsmere, I. Farrer, D.A. Ritchie, A. Tropper, A passively mode-locked external-cavity semiconductor laser emitting 60-fs pulses, Nat. Photon. 3 (2009) 729–731.

[5] M. Scheller, C.W. Baker, S.W. Koch, J.V. Moloney, Dual-Wavelength Passively Mode-Locked Semiconductor Disk Laser, IEEE Photon. Technol. Lett. 28 (12) (2016) 1325–1327.

[6] M.A. Gaafar, A.R. Iman, K.A. Fedorova, W. Stolz, E.U. Rafailov, M. Koch, Mode-locked semiconductor disk lasers, Adv. Opt. Photonics 8 (3) (2016) 370–400.

[7] M.A. Holm, D. Burns, A.I. Ferguson, M.D. Dawson, Actively Stabilized Single-Frequency Vertical-External-Cavity AlGaAs Laser, IEEE Photon. Technol. Lett. 11 (12) (1999) 1551–1553.

[8] M. Jacquemet, M. Domenech, G.L. Leclin, P. Georges, J. Dion, M. Strassner, I. Sagnes, A. Garnache, Single-frequency cw vertical external cavity surface emitting semiconductor laser at 1003 nm and 501 nm by intracavity frequency doubling, Appl. Phys. B 86 (2007) 503–510.

[9] A. Laurain, M. Myara, G. Beaudoin, I. Sagnes, A. Garnache, High power single–frequency continuously–tunable compact extended–cavity semiconductor laser, Opt. Express 17 (12) (2009) 9503–9508.

[10] A. Laurain, M. Myara, G. Beaudoin, I. Sagnes, A. Garnache, Multiwatt-power highly-coherent compact single-frequency tunable Vertical-External-Cavity-Surface- Emitting-Semiconductor-Laser, Opt. Express 18 (14) (2010) 14627–14636.

[11] A. Rantamäki, A. Chamorovskiy, J. Lyytikäinen, O. Okhotnikov, 4.6-W Single Frequency Semiconductor Disk Laser With <75-kHz Linewidth, IEEE Photon. Technol. Lett. 24 (16) (2012) 1378–1380.

[12] F. Zhang, B. Heinen, M. Wichmann, C. Möller, B. Kunert, A.R. Iman, W. Stolz, M. Koch, A 23-watt single-frequency vertical-external-cavity surface-emitting laser, Opt. Express 22 (11) (2014) 12817.

[13] T. Leinonen, Y.A. Morozov, A. Härkönen, M. Pessa, Vertical External-Cavity Surface-Emitting Laser for Dual-Wavelength Generation, IEEE Photon. Technol. Lett. 17 (12) (2005) 2508–2510.

[14] L. Fan, M. Fallahi, J. Hader, A.R. Zakharian, J.V. Moloney, W. Stolz, S.W. Koch, R. Bedford, J.T. Murray, Linearly polarized dual-wavelength vertical-external-cavity surface-emitting laser, Appl. Phys. Lett. 90 (2007), 181124.

[15] F. Zhang, M. Gaafar, C. Möller, W. Stolz, M. Koch, A.R. Iman, Dual-Wavelength Emission From a Serially Connected Two-Chip VECSEL, IEEE Photon. Technol. Lett. 28 (8) (2016) 927–929.

[16] P. Zhang, L. Mao, X. Zhang, T. Wang, L. Wang, R. Zhu, Compact dual-wavelength vertical-external-cavity surface-emitting laser with simple elements, Opt. Express 29 (11) (2021) 16572.

[17] R.K. Kim, S. Chu, Y.G. Han, Stable and Widely Tunable Single-LongitudinalMode Dual-Wavelength Erbium-Doped Fiber Laser for Optical Beat Frequency Generation, IEEE Photon. Technol. Lett. 24 (6) (2012) 521–523.

[18] Y. Zhang, C. Yang, Z. Feng, H. Deng, M. Peng, Z. Yang, S. Xu, Dual-wavelength passively q-switched single frequency fiber laser, Opt. Express 24 (14) (2014) 16149.

[19] G.Y. Hou, L.J. Wang, J. Feng, A. Popp, B. Schmidt, H.Y. Lu, C.Z. Tong, S.L. Shu, L. J. Wang, Near-diffraction-limited semiconductor disk lasers, Opt. Commun. 449 (2019) 39–44.

[20] Y. Zhang, L. Zhou, T. Zhang, Y. Cai, B. Xu, X. Xu, J. Xu, Blue diode-pumped single-longitudinal-mode Pr:YLF lasers in orange spectral region, Optics Laser Technol. 130 (2020), 106373.

[21] B. Xu, Y. Cheng, B. Qu, S. Luo, H. Xu, Z. Cai, P. Camy, J.L. Doualan, R. Moncorgé, InGaN-LD-pumped Pr^{3+}:$LiYF_4$ continuous-wave deep red lasers at 697.6 and 695.8 nm, Opt. Laser Technol. 67 (2015) 146–149.

[22] B. Xu, P. Camy, J.L. Doualan, A. Braud, Z. Cai, F. Balembois, R. Moncorgé, Frequency doubling and sum-frequency mixing operation at 469.2, 471, and 473 nm in Nd:YAG, J. Opt. Soc. Am. B 29 (3) (2012) 346–350.

[23] S.J. Fu, W. Shi, H.W. Zhang, Q. Sheng, G.N. Shi, X.L. Bai, J.Q. Yao, Linewidth-narrowed, linear-polarized single-frequency thulium-doped fiber laser based on stimulated brillouin scattering effect, IEEE Photon. J. 9 (4) (2017) 1504207.

[24] J.L. Lan, Y. Wang, X.X. Huang, Z. Lin, B. Xu, H.Y. Xu, Z.P. Cai, X. Xu, J. Xu, Single- and dual-wavelength lasers of diode-pumped Nd:LuYAG mixed crystal on various $^4F_{3/2} \rightarrow {}^4I_{13/2}$ Stark-level transitions, J. Phys. D: Appl. Phys. 49 (2016), 305101.